

What the Clinician Wants to Know

Charles A. Goldfarb, MD
Yuming Yin, MD
Louis A. Gilula, MD
Andrew J. Fisher, MD
Martin I. Boyer, MD

Index terms:
Bones, CT, 43.1211
Wrist, fractures, 43.41
Wrist, MR, 43.12141, 43.121415
Wrist, radiography, 43.11

Radiology 2001; 219:11–28

Abbreviations:

AO = Association for the Study of Internal Fixation
AVN = avascular necrosis
DRUJ = distal radioulnar joint
PA = posteroanterior
TFC = triangular fibrocartilage
TFCC = TFC complex

¹ From the Mallinckrodt Institute of Radiology, Washington University School of Medicine, 510 S Kingshighway Blvd, St Louis, MO 63110 (Y.Y., L.A.G.); the Department of Orthopaedic Surgery, Washington University Medical School, St Louis, Mo (C.A.G., M.I.B.); and Radiology Imaging Associates, Englewood, Colo (A.J.F.). Received March 23, 1999; revision requested May 21; revision received December 28; accepted February 1, 2000. Address correspondence to L.A.G. (e-mail: gilula@mir.wustl.edu). © RSNA, 2001

Wrist Fractures: What the Clinician Wants to Know¹

With the recent improvements in diagnosis and treatment of distal radius and carpal injuries, the hand surgeons' expectations of relevant radiologic interpretation of imaging studies are heightened. Conventional radiographic examinations, as well as more sophisticated and invasive studies, have important roles in the evaluation of wrist fractures and dislocations. On the basis of physical examination results and the mechanism of injury, the onus is on the examining surgeon to pinpoint potential sites of bone or ligament disruption. After this evaluation, appropriate imaging studies appropriately performed and interpreted will help direct treatment and improve outcome with greater clarity and certainty.

While the orthopedic surgeon and the emergency medicine physician initially evaluate injuries of the wrist, which includes the distal radius, distal ulna, carpal bones, and metacarpal bases, it is the radiologist who confirms a clinical suspicion of injury and further characterizes the nature of this injury. To seamlessly integrate care, the radiologist must possess an understanding of the factors that alter clinical decision making and patient treatment. The radiologic report should, therefore, contain all the information a clinical colleague requires to determine patient disposition and should use language common to both specialties.

Full evaluation requires more than simple fracture detection and description. Pertinent ancillary findings and negative radiographic findings that factor into clinical algorithms must be addressed. It is important that radiographs be inspected with the knowledge of injury mechanism as it relates to future care, potential fracture complications, and consequent implications.

DISTAL RADIUS FRACTURES

Fractures of the distal radius account for an estimated 17% of fractures seen acutely in the emergency department (1). These injuries occur most commonly among elderly women with osteoporosis, typically because of a fall onto an outstretched hand. Younger patients may also sustain distal radius fractures, often caused by a high-energy mechanism such as a motor vehicle accident, and these patients may have additional orthopedic injuries. Despite the high frequency of these fractures, indications for surgical intervention and the method of treatment remain somewhat subjective. Although results from numerous clinical and laboratory studies (2–6) have aided the understanding of these complex injuries, further investigation is necessary.

The goal in treating distal radius fractures is the rapid restoration of function, with attention given to the prevention of chronic disability. This involves diagnosis, appropriate intervention, and postintervention rehabilitation. The key element in the treatment algorithm is the development of a functional understanding of the injury, beginning with an appreciation of the local anatomy, injury pattern, and associated injuries.

Anatomy

Both the radiocarpal articulation and the distal radioulnar joint (DRUJ) must be considered when evaluating fractures of the distal radius. The distal radius has three concave surfaces: the scaphoid and lunate fossae, which articulate with the named carpal bones, and the sigmoid notch, which articulates with the ulna at the DRUJ (Fig 1). The metaphyseal widening of the distal radius begins approximately 2 cm proximal to the radiocarpal joint. Distal to this broadening, the amount of cortical bone decreases, and the corre-

sponding amount of weaker cancellous bone increases, forming a zone predisposed to fracture.

The DRUJ consists of the concave sigmoid notch of the distal radius, the distal ulna, and the supporting capsuloligamentous structures. It is supported by the structures of the triangular fibrocartilage complex (TFCC), which includes a fibrous meniscus-like structure (the triangular fibrocartilage [TFC]), which runs from the sigmoid notch to the ulnar styloid and the surrounding soft-tissue attachments. The TFCC supports the articulation of the distal ulna with both the lunate and triquetrum. Ulnar-sided wrist pain in the absence of radiographic evidence of fracture must raise the suspicion of an injury to the TFCC. The radiocarpal and the intercarpal articulations are supported by the radiocarpal ligaments, and the origins and insertions of these ligaments must be considered when evaluating fractures of the distal radius or carpus (8) (Fig 2).

Imaging Assessment

A radiographic survey of the distal radius and ulna can be accomplished with simple posteroanterior (PA) and lateral views; however, we recommend a four-view series for a more complete evaluation of the wrist. This includes PA and lateral views, an external oblique projection, and a PA view with the wrist in ulnar deviation. An external oblique view is obtained with the radial side of the wrist elevated at a 30° angle off the table or film screen, with the ulnar side of the hand and wrist on the table. The external oblique view is the only one of these survey views that demonstrates the trapezio(trapezoidal joint; it also demonstrates the waist of the scaphoid. Placement of the wrist in ulnar deviation while in the PA position elongates the scaphoid and helps improve detection of subtle scaphoid fractures (10). Standardized positioning and high-quality radiographs must be obtained for optimal evaluation at the time of injury and subsequent follow-up. We prefer to perform a three-view examination of the wrist at follow-up when the wrist is in a cast, without obtaining the ulnar-deviated PA view. It could be argued that only PA and lateral views should be obtained at follow-up, but follow-up studies to show the entire wrist on four views whenever possible will enable detection of additional abnormalities not shown at first. Examples of this would be a developing scapholunate dissociation, an increasing

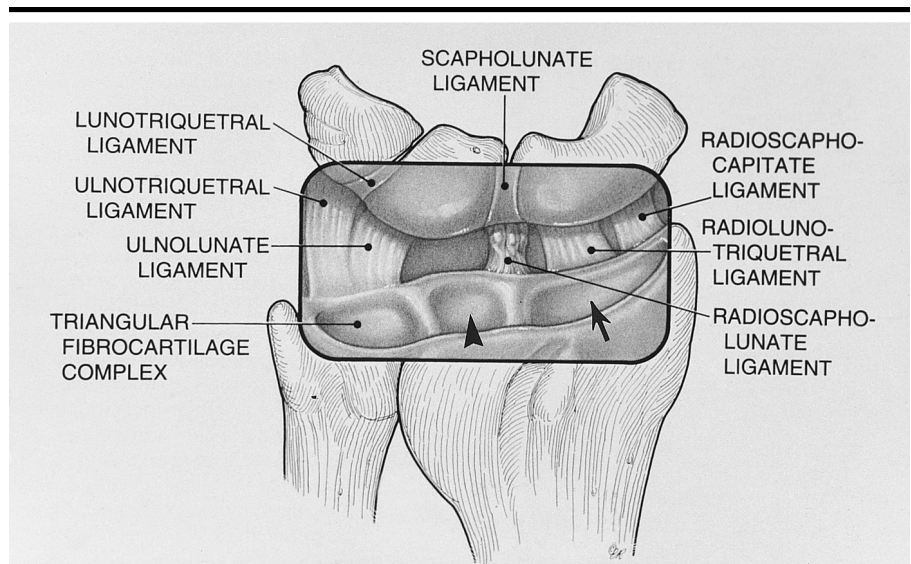


Figure 1. Anatomic diagram shows the radiocarpal joint with fossae to articulate with the scaphoid (scaphoid fossa) (arrow), lunate (lunate fossa) (arrowhead), and ulnar side of the carpus. (Modified and reprinted, with permission, from reference 7.)

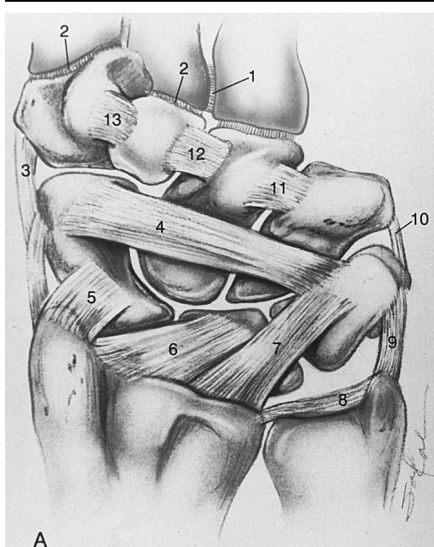
fracture-fragment displacement, and detection of additional fractures or displacements not seen originally.

A standard PA view of the wrist should profile the extensor carpi ulnaris tendon groove, which should be at the level of or radial to the base of the ulnar styloid (11). A true lateral view is defined by a scaphopisocapitate relationship (12). On a standard lateral view, the palmar cortex of the pisiform bone should overlie the central third of the interval between the palmar cortices of the distal scaphoid pole and the capitate head (Fig 3). These two criteria provide an objective measure of true standard PA and lateral views.

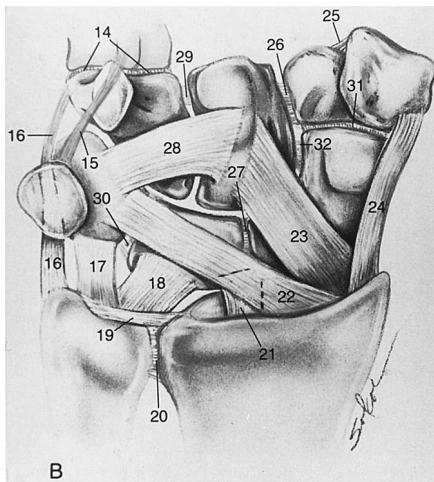
When evaluating radiographs in patients with a high potential for a fracture, the bone cortices must be carefully evaluated for evidence of discontinuity. One must evaluate both the PA and the lateral views because a subtle fracture may be apparent on only one view (Fig 4). On the PA view, cortices of the scaphoid, lunate, and sigmoid fossae of the distal radius should be carefully examined for cortical offset. On the lateral view, all cortical structures, including the distal radius, the ulna, the carpal bones, and the metacarpal cortices, should be examined carefully for cortical break. Soft-tissue swelling must also be carefully assessed. With focal swelling, close observation of underlying cortices may show a fracture or subluxation. The distal ulna should also be closely evaluated when a distal radioulnar subluxation or dislocation is considered.

With fracture comminution, displacement, or complex intraarticular extension, radiography may be insufficient and computed tomography (CT) is warranted. CT should be performed if conventional radiographs provide insufficient detail and, specifically, when a detailed evaluation is needed of radiocarpal articular step-off and gap displacement—factors crucial in predicting the development of radiocarpal osteoarthritis (2,13).

CT of the distal radius, ulna, and carpus can be performed in several planes. CT in the transverse plane is often used to evaluate the distal radioulnar joint and the carpal bones or to further assess a longitudinal fracture. The coronal plane provides an image similar to the standard PA radiograph but will provide better soft-tissue and bone detail than will a routine radiograph. Coronal CT also demonstrates the radiocarpal joint well. The oblique sagittal plane in the long axis of the scaphoid was developed to better assess the scaphoid. The wrist is pronated and the scans are obtained along a line between the base of the thumb and the Lister tubercle (dorsal tubercle of radius) (14). In subtle cases of distal radioulnar subluxation, a comparison of transverse CT images of both wrists in the neutral, prone, and supine positions or in any position that reproduces the patient's pain may be helpful (14). In general, 2-mm-thick sections at 2-mm intervals will be satisfactory to show the anatomic detail of distal radius



A



B

Figure 2. (a) Schematic shows dorsal view of the wrist joint. 1 = dorsal intermetacarpal ligament, 2 = dorsal carpometacarpal ligament, 3 = radial collateral ligament, 4 = dorsal intercarpal ligament, 5 = pars radioscapoid of the dorsal radiocarpal ligament, 6 = pars radiolunate of the dorsal radiocarpal ligament, 7 = pars radiotriquetrum of the dorsal radiocarpal ligament, 8 = TFC, 9 = ulnar collateral ligament, 10 = ulnar collateral ligament, 11 = capitohamate ligament, 12 = trapezoidocapitate ligament, 13 = trapeziotrapezoid ligament. (b) Schematic shows volar view of wrist joint. 14 = volar carpometacarpal ligament, 15 = pisohamate ligament, 16 = ulnar collateral ligament, 17 = ulnotriquetral ligament, 18 = ulnolunate ligament, 19 = triangular fibrocartilage, 20 = capsule of distal radioulnar joint, 21 = volar radioscapolunate ligament, 22 = volar radiolunotriquetral ligament, 23 = volar radiocapitate (radioscaphocapitate) ligament, 24 = radial collateral ligament, 25 = trapeziotrapezoid ligament, 26 = trapezoidocapitate ligament (intercarpal capsular and interosseous), 27 = scapholunate interosseous ligament, 28 = volar capitotriquetral ligament, 29 = capitohamate ligament, 30 = lunotriquetral interosseous ligament, 31 = scaphotrapeziotrapezoidal intercarpal capsular ligament, 32 = scaphocapitate intercarpal capsular ligament. (Reprinted, with permission, from reference 9.)

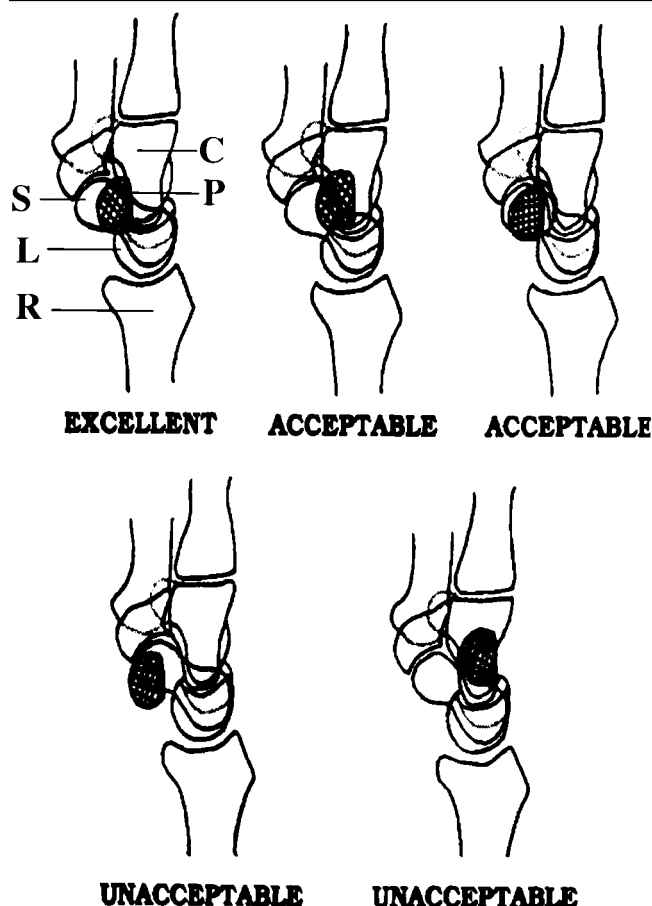


Figure 3. Illustration of the scaphopisocapitate criterion for lateral wrist alignment. The ventral cortex of the pisiform bone (P) should lie between the ventral cortices of the distal pole of the scaphoid (S) and the head of the capitate (C). When the ventral cortex of the pisiform bone is outside of these borders, lateral alignment is unacceptable. The bone with hatch marks is the pisiform bone. L = lunate, R = radius. (Reprinted, with permission, from reference 12.)

and ulnar fractures along articular surfaces. When evaluating carpal bone fractures and displacements, it is sometimes of value to add 2-mm-thick sections at 1-mm intervals in one plane for more anatomic detail, as for a scaphoid fracture. We prefer not to use reconstructed images for a second plane, unless prior use of a scanner shows that the machine can produce excellent-quality reconstructed images that equal the quality of directly acquired images.

Magnetic resonance (MR) imaging is of benefit when concomitant ligamentous injuries are suspected or if fracture is suspected but not demonstrated on routine radiographs (15). MR imaging should provide images in at least the transverse and coronal planes, and at least one sequence sensitive for fluid with fat suppression should be included. Section thickness should preferably be 3 mm or

less for evaluation of bone marrow. Thinner sections are necessary for ligament evaluation. Arthrography is valuable when looking for scapholunate, lunotriquetral, TFC, or TFCC defects (16).

Standard radiographic assessment to quantify deformities associated with distal radius fractures should also consist of three radiographic measurements, which correlate with patient outcome (Fig 5) (4,17). Radial length (radial height) is measured on the PA radiograph as the distance between one line perpendicular to the long axis of the radius passing through the distal tip of the sigmoid notch at the distal ulnar articular surface of the radius and a second line at the distal tip of the radial styloid. This measurement averages 10–13 mm. Radial inclination, or radial angle, is also measured on the PA radiograph and represents the angle between one line connecting the ra-

dial styloid tip and the ulnar aspect of the distal radius and a second line perpendicular to the longitudinal axis of the radius. The radial inclination ranges between 21° and 25°. The volar tilt of the distal radius (19) is measured on a correctly positioned lateral radiograph (12). The volar tilt represents the angle between a line along the distal radial articular surface and the line perpendicular to the longitudinal axis of the radius at the joint margin. The normal volar tilt averages 11° and has a range of 2°–20°. The importance of these measurements will be discussed in following sections.

Classification

A worthwhile classification system should be easy to apply, assist with prognosis, and aid in treatment. Several classification systems for distal radius fractures are currently in use, but an accurate description, with the salient features as outlined subsequently, is often favored over the use of these systems. A list of common eponyms is provided, because these terms are commonly used in clinical practice.

A Colles fracture (20) is a transverse fracture of the distal radial metaphyseal area with dorsal angulation and displacement of the distal fragment (Fig 6). This is the most common fracture of the distal radius and is typically produced by a fall on an outstretched hand, with the wrist dorsiflexed. Radiocarpal and DRUJ extension of the fracture line(s), radial shortening, loss of radial inclination and palmar tilt, and ulnar styloid fractures are often observed; these are the key radiographic features to be looked for and will be discussed more fully subsequently.

A Smith fracture (21) is a reversed Colles fracture in which the fracture of the metaphyseal area demonstrates volar angulation of the distal fracture fragment (Fig 7). Typically, Smith fractures occur in younger patients and are the result of from higher energy trauma on the volar flexed wrist. Volar comminution is common.

A Barton fracture (22) implies a shear type fracture of the distal articular surface of the radius with translation of the distal radius fragment with the carpus. The volar (Fig 8) and dorsal subtypes are distinguished by the location of the fracture fragment and the direction of displacement of the radius fragment and the carpus with respect to the radius proper. Rarely, dorsal comminution may be present with a volar Barton injury or volar comminution with a dorsal Barton injury. This complex injury



Figure 4. (a) PA radiograph of the left wrist demonstrates a normal appearance. (b) Lateral radiograph of the same wrist demonstrates a chip fracture (arrow) from the dorsal aspect of the triquetrum.

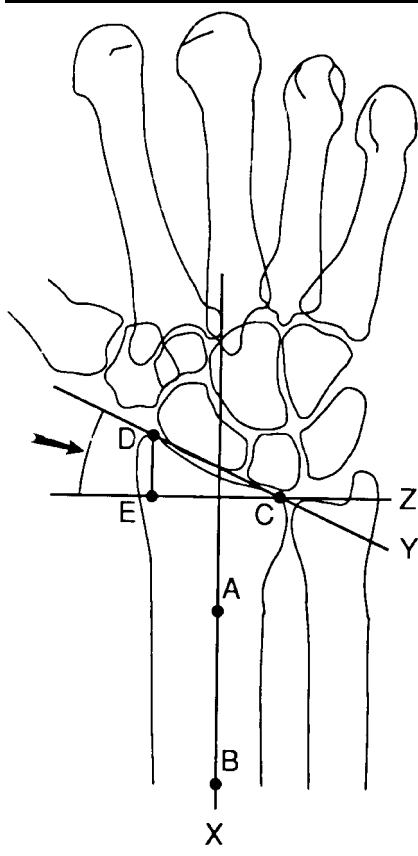
is typically related to transverse loading with a shearing component.

A Hutchinson (chauffeur) fracture (23) consists of an oblique, intraarticular fracture of the distal radius. The radial styloid is within the fracture fragment, although the fragment can vary markedly in size. Potential displacement is associated with the intercarpal ligamentous attachments of the fragment. Furthermore, there may be associated intercarpal ligamentous injuries, especially of the scapholunate ligament. The term "chauffeur" originates from injuries sustained while using automobile crank starters in the early 20th century. This fracture is typically a shear or translational injury with forces transmitted through the scaphoid or scapholunate joint.

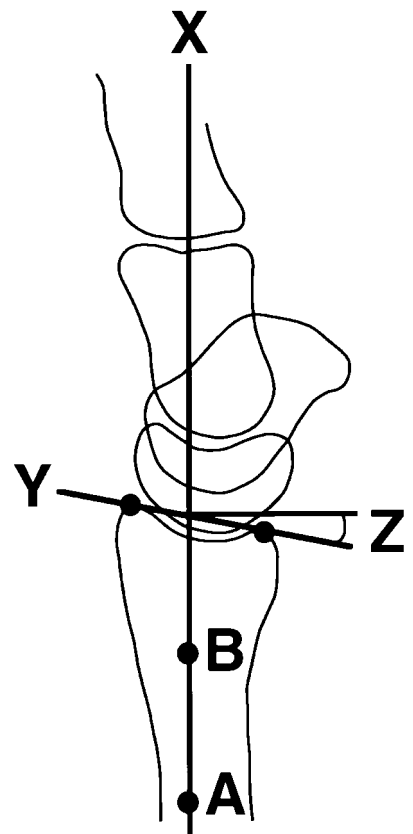
A die-punch fracture (24) typically occurs in the lunate fossa of the distal radius (Fig 9). A transverse load is transmitted through the lunate, resulting in a depressed fracture of the articular surface of the distal radius. The subtle depressed fracture of the lunate fossa may be easily overlooked, but an understanding of the carpal arcs as seen on the PA view of the wrist will often assist in identification of a carpal fracture or ligamentous injury. Carpal arc I is defined as a smooth curve that connects the outer proximal convexities of the scaphoid, lunate, and triquetrum. Carpal arc II is a smooth arc that joins the distal concavity of these same three carpal bones. Carpal arc III is a smooth curve that joins the proximal convexities of the capitate and hamate.

Arches are evaluated in the neutral position; that is, with the third metacarpal shaft coaxial with the radius shaft (10,25). A break in these arcs is suggestive of an abnormality at the site of the broken arc (Fig 9).

Individual physicians find merit in different classification schemes. It has been recognized that inter- and intraobserver reliability for fracture classification among radiologists and orthopedic surgeons is poor, which adds to the diagnostic and therapeutic confusion over treatment of wrist fractures (26). Nevertheless, knowledge of major classification systems helps the radiologist understand thought processes of the diagnosing and treating hand surgeon. The four most commonly used classification systems include the Frykman, Melone, AO (Association for the Study of Internal Fixation), and Fernandez and Jupiter classifications. The Fernandez and Jupiter classification addresses the mechanism of injury, is preferred by many, and will serve as the basis for our discussion of treatment options. At each imaging center, preferences of the treating hand surgeon should be known, so that the radiologist can utilize the preferred classification system. Nevertheless, each of the classification systems has its advantages. The radiologist must identify the major abnormalities in each classification system that can influence decision making about treatment. The important abnormalities stressed in all the classification systems include intraarticular involvement of the scaphoid and lunate fossae, sigmoid notch, and ul-



a.



b.

Figure 5. (a) Schematic shows method for determination of radial height (radial length) (normal measure, 10–13 mm), which is the measured distance between points D and E, where D represents the distal-most tip of the radial styloid and E is a point on line EC. Line DE is the shortest distance between point D and line EC. Radial inclination angle (arrow) is measured by drawing a perpendicular line (line EC) to the radial axis (AB) through the distal sigmoid notch (the ulnar edge of the lunate fossa) and by drawing another line (line DC) joining the distal tip of the radial styloid and the distal sigmoid notch (ulnar edge of the lunate fossa). These two lines form the radial inclination angle (normal angle, 21°–25°). (b) Schematic shows the palmar (volar) tilt, which is the angle created between the line (Y) joining the most distal points of the dorsal and ventral rims of the distal articular surface of the radius and the line (Z) drawn perpendicular to the long axis (line XBA) of the radius. The average tilt is 11°, with a range of 2°–20°. (Modified and reprinted, with permission, from reference 18.)

nar styloid. The site of the ulnar styloid fracture should also be identified. Fractures at the base of the ulnar styloid are more likely to be associated with avulsions of the TFC than with avulsions of the most distal tip of the ulnar styloid (27).

The Frykman classification (Fig 10), published in 1967 (28), is rarely used today but bears mention because it was the first classification to note the importance of DRUJ extension of the fracture lines and ulnar styloid involvement. This classification system notes four fracture patterns: extraarticular metaphyseal, intraarticular extension to the radiocarpal joint, intraarticular extension to the DRUJ, and intraarticular extension involving both joints. The presence of ulnar styloid involvement is also incorporated.

The Melone classification (Fig 11), published in 1986 (29), categorizes distal radius fractures on the basis of the number of parts: shaft, styloid, dorsal medial facet, and volar medial facet. The current modified classification adds a fifth group of severely comminuted fractures. The importance of the radiolunate articulation is emphasized in this classification.

The AO classification is organized into three groups—A, B, and C—on the basis of fracture severity. These groups are subdivided into numbered divisions on the basis of articular involvement or lack thereof: extraarticular, partial articular (fractures in which part of the distal radius articular surface remains in continuity with the radius itself), and intraarticular. With the full AO classification, there are 27 potential fracture patterns,

and the interobserver agreement for this classification is poor. However, when only the A, B, and C groups are used, more consistent agreement between physicians can be expected (26).

The final system is the Fernandez and Jupiter, or mechanistic, classification system (Fig 12) (31). Any organization based on mechanism is certain to be of assistance in treatment because knowledge of deforming forces is critical in determining appropriate intervention. This classification system closely mirrors prognosis; fracture forces and subsequent comminution progressively increase from type I to type V, and outcome concomitantly worsens. Type I fractures are bending fractures and include metaphyseal Colles and Smith fractures. These are caused by tensile volar or dorsal loading, respectively, with subsequent comminution of the opposite cortex (Figs 6, 7). Type II fractures are shear fractures of the joint surface and include volar and dorsal Barton injuries (Fig 8). Type III fractures are compression fractures of the articular surface and include die-punch fractures. Type IV fractures are avulsion fractures and are associated with radiocarpal fracture-dislocations. These fractures include radial and ulnar styloid injuries. Type V fractures are high-velocity injuries with comminution and often with bone loss. They are related to a complex interaction of multiple forces.

Treatment

The treatment of distal radius fractures involves an extensive algorithm with many acceptable options. These options include (a) closed reduction; (b) closed reduction with percutaneous pinning, or CRPP; (c) CRPP and external fixation, with or without bone grafting; (d) closed reduction and external fixation; (e) open reduction with percutaneous pinning; (f) open reduction with plate fixation; (g) open reduction with external fixation; (h) limited open reduction (lunate facet) with percutaneous pinning; (i) limited open reduction (lunate facet) with plate fixation; and (j) limited open reduction (lunate facet) with external fixation.

Basic treatment parameters will be discussed in relation to the mechanistic classification. Several general factors must be considered. The age of the patient is important to consider, because a reduction that is acceptable in a retired, sedentary, elderly patient may be unacceptable in a young laborer. Decisions on appropriate treatment must focus on the demand, hand dominance, and bone quality required for

surgical fixation. Associated injuries must also be considered. Multiple injuries and open fractures often warrant immediate intervention, whereas most other injuries may be treated with closed reduction at the emergency department, and surgical intervention, if necessary, can be scheduled on a semi-elective basis.

The initial treatment for most distal radius fractures is closed reduction and plaster immobilization. An effective reduction depends on relaxation of the local musculature with adequate analgesia. To block the pain-muscle spasm feedback loop, a hematoma block—*injection of several milliliters of local anesthetic into the fracture site*—is administered. Any reduction maneuver must begin with longitudinal traction for several minutes to assist in muscle relaxation. Next, the injury is recreated to aid in unlocking the fracture fragments, and then the deformity is reversed for reduction. Once reduced, the fracture must be splinted in a fashion to maintain the reduction. The splint is typically molded in a fashion to reverse the displacing forces with three points of pressure. A Colles fracture would be splinted with volar pressure at the fracture site and dorsal pressure just proximal and distal to the fracture site. Repeat radiographs are then obtained to evaluate the restoration of radial length, inclination, volar tilt, and articular congruity, along with the presence and severity of associated comminution.

Fracture comminution and intraarticular involvement are common and must be addressed in the radiographic report. Aside from location of the comminution and intraarticular involvement, which should correspond to the mechanism of the injury, the report should attempt to quantify the comminution. Extensive comminution makes fracture reduction and maintenance of reduction more difficult because of the loss of bone stability. For similar reasons, it makes surgical reduction more challenging.

If an anatomic reduction is performed, the patient is seen within 1 week for repeat radiography. Patients are generally not treated with a cast in the emergency department because of the potential complications related to swelling such as skin breakdown or compartment syndrome. Cast placement may be performed at the initial follow-up if radiographic findings confirm maintenance of reduction. Patients are typically seen again 1 week after cast placement, and close follow-up is mandatory to ensure that fracture reduction is not lost. Surgi-



Figure 6. Colles fracture. (a) PA radiograph of the right wrist demonstrates a comminuted intraarticular fracture of the distal radius with a proximal and ulnar shift of the carpus relative to the radius. (b) Lateral radiograph of the same wrist demonstrates a distal radius fracture with the distal fracture fragments displaced and angled dorsally relative to the proximal fracture fragment.

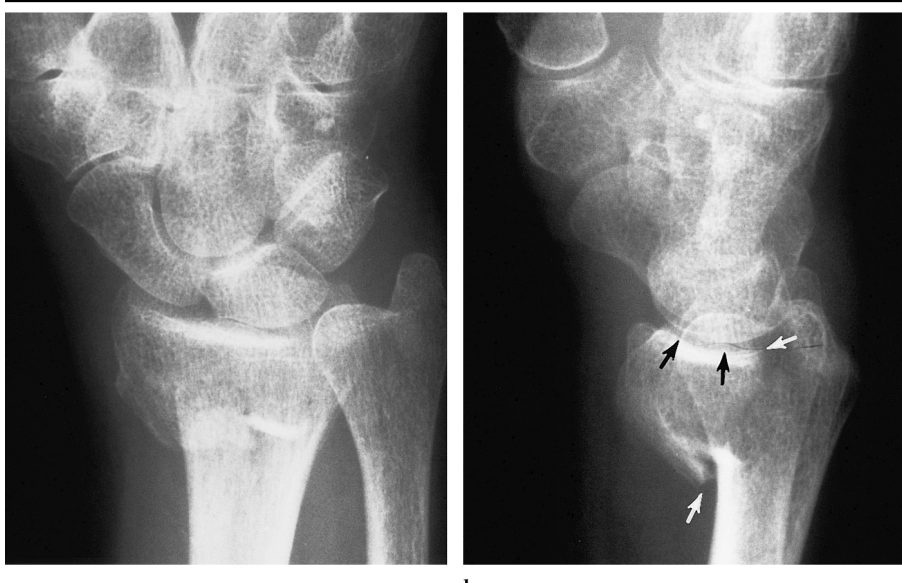


Figure 7. Smith fracture. (a) PA radiograph of the left wrist demonstrates a transverse comminuted fracture of the distal radius. (b) Lateral radiograph of the same wrist demonstrates a comminuted distal radius fracture (between arrows) with the distal fracture fragment displaced and angled in the palmar direction relative to the proximal fracture fragment. The distal articular surface of the radius has an abnormally increased palmar tilt.

cal intervention is usually required when there is failure to obtain or maintain closed reduction during the time needed for osseous union. At each follow-up, the evaluation of the articular surface, radial length, radial inclination, and volar tilt should be addressed. Compromise in the maintenance of the reduction will be noted and quantified with a change in

any one of these values. Nonunion is rare with these injuries, in large part because of the excellent blood supply of the distal radius, and malunion is the more common complication.

Fernandez and Jupiter type I fractures with dorsal angulation of the distal radius fragment (Colles fractures) can be treated with a dorsal-radial splint with



a.

b.

Figure 8. Reverse (volar) Barton fracture. (a) PA radiograph of the right wrist demonstrates a comminuted intraarticular fracture of the distal radius with the distal fracture fragment migrated proximally and radially. (b) Lateral radiograph of the same wrist demonstrates an intraarticular fracture of the distal radius with the volar fragment (arrows) maintaining its relationship with the carpus. The volar fracture fragment and carpus have migrated proximally relative to the dorsal fracture fragment and shaft of the radius.

standard three-point pressure to reverse the forces of the mechanism of injury. A three-point mold for a Colles fracture has one dorsal point of molding at the apex of angulation and two volar points of molding, one just distal and one just proximal to the fracture. The molding of the cast will resist displacement by reversing the deforming forces. Likewise, type I fractures with volar angulation of the distal radius fragment (Smith injuries) can be treated with a volar-radial splint in most instances. Those with severe comminution are more likely to displace and may require either repeat reduction or surgical intervention, depending on radiographic findings at repeat imaging. Comminution and/or osteoporotic bone often make external fixation the preferred surgical treatment option. Surgery can be combined with percutaneous pinning for stability. Percutaneous pinning with plaster support may also be chosen, but there are many associated complications (32). External fixation provides stability but has numerous potential side effects, including patient dissatisfaction, infection, joint stiffness, and atrophy. Rarely is open reduction with plate fixation necessary for these extraarticular fractures.

Type II fractures (Barton fractures) may be treated by means of closed reduction and splinting, but because of the shearing nature of the injury, closed reduction is rarely successful. Therefore, volar Bar-

ton fractures are treated with a volar buttress plate, and dorsal Barton fractures are treated with a dorsal plate. Associated styloid injuries can be percutaneously pinned.

Type III injuries can often be treated with closed reduction and a cast. With these injuries, careful evaluation of the postreduction radiographs, including oblique views, is paramount. Any suspicion of articular incongruity warrants CT for further evaluation of fragment displacement. If a step-off greater than 2 mm and/or a gap deformity exists, limited open reduction and percutaneous pinning may be sufficient to restore the articular surface (33). Limited open reduction prevents extensive scarring and allows an average of 20° of increased wrist motion when compared with that after standard open reduction. Extensive comminution may necessitate bone grafting and, potentially, external fixation for support. Extensive comminution may be defined as multiple fragments, especially when small. The extent of comminution and the determination of size of fracture fragments, with regard to suitability of internal fixation, can be determined with CT images (13). Some of these fractures are treated with surgical reduction and internal fixation.

Type IV injuries are associated with radiocarpal fracture-dislocations. Percutaneous pinning of the styloid fractures after closed reduction may be sufficient; occasionally, however, ligamentous or capsular

repair may be necessary. Ulnar styloid fractures must be noted, because these injuries may indicate injury to the TFCC, depending on the level of the styloid fracture. The larger the fragment of the ulnar styloid, the greater the chance of injury to the TFCC (27). Because the ulnar edge of the TFC attaches to the ulnar styloid, the entire TFC and TFCC may be avulsed from the ulna with a fracture through the base of the ulnar styloid. Anatomic reduction and pinning may be necessary if a large styloid fragment is involved or if an old healed one is symptomatic.

Type V injuries are comminuted, and, although closed reduction should be attempted, surgical treatment is generally required. If radial length can be restored and articular congruity maintained with external fixation alone, no other intervention is necessary. Often, bone grafting and/or percutaneous pinning must be combined with external fixation. Severe comminution requires open reduction and internal fixation.

DISTAL RADIUS MALUNION

The incidence of distal radius malunion, or fracture healing in a nonanatomic position has been estimated to be 23%, but symptomatic malunion is less frequent (34). The senior orthopedic surgeon author of this article (M.I.B.) believes that the term "malunion" can be applied to any fracture with a dorsal tilt of 5° or greater, a radial inclination of 10° or less, or a loss of 5 mm or more of radial height. The authors of numerous studies (35,36) have assessed distal radius fractures and the development of malunion in an effort to better understand which one or more of these radiographic parameters are most relevant for outcome. Currently, there is no consensus about which one parameter is the most specific predictor of symptomatic malunion. Therefore, radial length, radial inclination, volar tilt, and articular congruity must all be evaluated with each distal radius fracture, and anatomic reduction must be attempted in an effort to restore each parameter to baseline. Postreduction radiographic reports should include an assessment of these variables. When more clear detail about distal radius fractures than can be seen with conventional radiographs is desired, it has been shown that CT provides better information about fracture characteristics than does conventional radiography (2,13). CT sections should be obtained at right angles to fracture lines to best define fracture characteristics (14). Extraarticular and intra-

ticular malunion may manifest in distinct manners.

Patients with extraarticular malunion may be asymptomatic or complain of decreases in grip strength, wrist range of motion, and forearm supination and/or pronation or of pain and disability. The amount of anatomic variation required to develop symptoms varies substantially. Pogue et al (5) reported that normal wrist mechanics were maintained if radial shortening was less than 2 mm, volar tilt changed by less than 20°, and radial inclination was maintained at more than 10°. Conversely, a dorsal tilt of greater than 20°, a radial inclination of less than 10°, and a loss of radial height have all been associated with decreased function. The adverse outcome associated with malunion is related to altered loading patterns and the development of premature osteoarthritis.

Volar tilt is thought by many to be an important aspect of radial malunion (34). Dorsal angulation causes loss of wrist flexion and alters DRUJ mechanics. Dorsal angulation is associated with a dorsal shift in pressure transmission from the scaphoid and lunate to the radius. In addition, functional radial shortening is created with loss of volar tilt, and there is an associated increase in load transmission through the distal ulna. A change from 11° of volar tilt to 45° of dorsal tilt leads to an increase in ulnar loading from 18% of transmitted forces to 65% of forces (6). There is no universally acceptable amount of dorsal tilt, despite many studies on the subject; however, many orthopedic surgeons believe intervention is necessary in the presence of 10° of dorsal tilt (a change of 20° from the normal), although the age of the patient is crucial in this decision process (35). The radiologist should recognize the amount of volar or dorsal tilt of the distal radius, and the treating surgeon must make the clinical decision whether to intervene to try to change this alignment.

Others suggest radial shortening may be the most important factor in the development of symptomatic malunion. Normally, 80% of forces are borne through the radius, and 20% are borne through the ulna. Radial shortening as minimal as 2.5 mm can substantially complicate this dynamic and markedly increase ulnar loading (37). Shortening of 6 mm can lead to clinical manifestations (5). Radial shortening affects DRUJ mechanics and is associated with DRUJ osteoarthritis. Injury to the TFCC, loss of forearm rotation, and ulnocarpal impingement can result.

Loss of radial inclination is less impor-

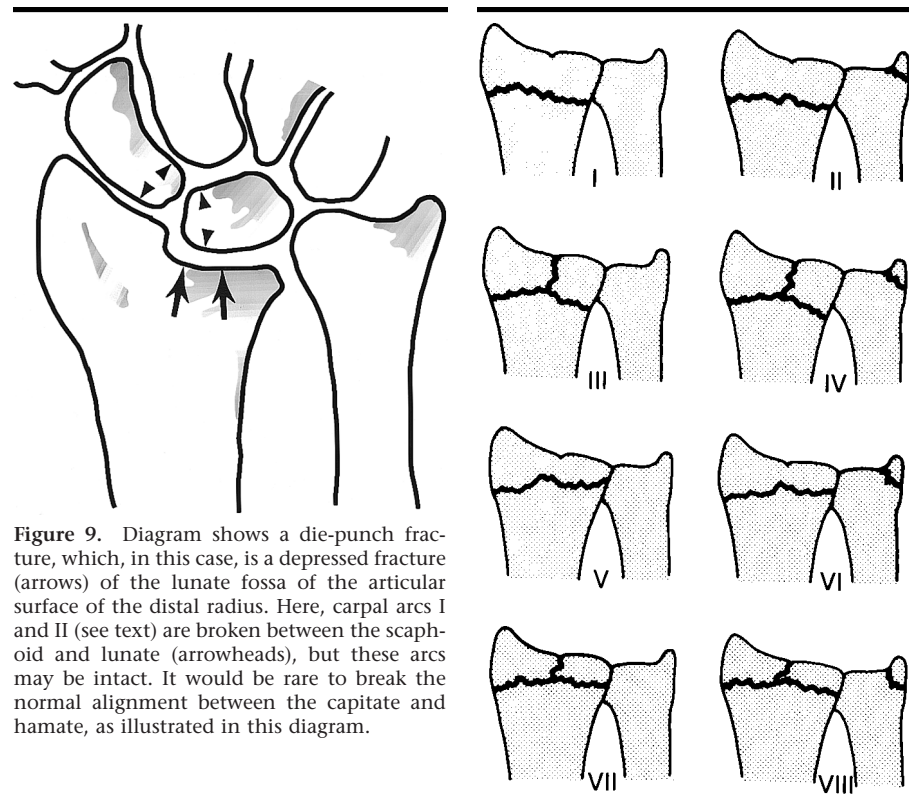


Figure 9. Diagram shows a die-punch fracture, which, in this case, is a depressed fracture (arrows) of the lunate fossa of the articular surface of the distal radius. Here, carpal arcs I and II (see text) are broken between the scaphoid and lunate (arrowheads), but these arcs may be intact. It would be rare to break the normal alignment between the capitate and hamate, as illustrated in this diagram.

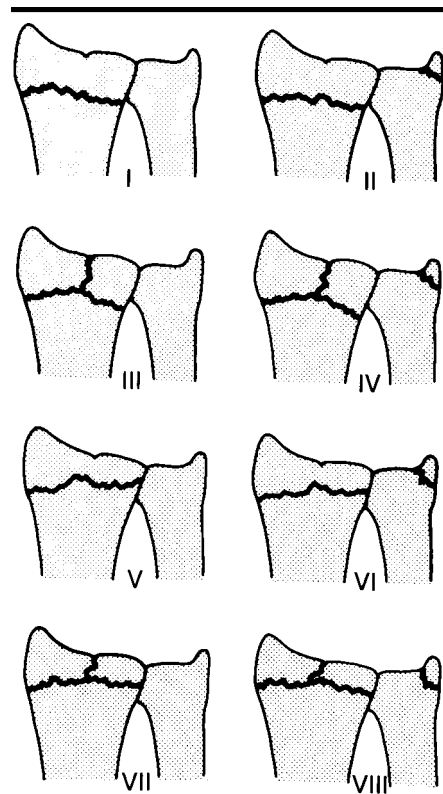


Figure 10. Diagram shows the Frykman classification of distal radius fractures with or without involvement of the ulnar styloid: type I, simple metaphyseal area fracture; type II, simple metaphyseal area fracture and ulnar styloid fracture; type III, metaphyseal area fracture with radiocarpal joint extension; type IV, metaphyseal area fracture with radiocarpal joint extension and ulnar styloid fracture; type V, metaphyseal area fracture with DRUJ extension; type VI, metaphyseal area fracture with DRUJ extension and ulnar styloid fracture; type VII, metaphyseal area fracture with DRUJ and radiocarpal extension; type VIII, metaphyseal area fracture with DRUJ and radiocarpal extension and ulnar styloid fracture. (Modified and reprinted, with permission, from reference 7.)

tant in the development of symptomatic malunion but may cause symptoms. Decreased ulnar deviation; loss of radial length, with its attendant problems; and diminished grip strength can develop with a 5°–10° loss of inclination (30). Furthermore, loss of radial inclination and radial length disrupt normal DRUJ function.

Whereas volar tilt, radial inclination, and radial height all contribute to symptomatic extraarticular malunion, intraarticular incongruity has its own complications. Articular incongruity is the most important factor in the development of posttraumatic osteoarthritis of the wrist. Catalano et al (2) found that both step and gap displacements of the distal radius are associated with premature osteoarthritis, with step deformity the more important parameter. However, despite radiographic evidence of osteoarthritis at 7.1-year follow-up, all patients with open reduction and internal fixation were clinically asymptomatic. Knirk and Jupiter (38) reported that 91% of patients with at least 2-mm articular incongruity will develop osteoarthritis, whereas only 11% of those with less than 2 mm of articular step and gap displacement will develop osteoarthritis. These findings highlight the importance of quantifying articular incongruity. CT may, therefore, be warranted for initial assessment and surgical planning for treatment of intraarticular fractures.

In summary, fractures of the distal radius are complex entities that have been the subject of extensive study and debate. A greater understanding of the nature of these injuries and of the treatment options have allowed the radiologist to have a more substantive effect on patient care. It is important, therefore, that the radiographic reports be directed at detailing the fracture and its potential intraarticular extensions, as well as the important variables of radial length or height, radial inclination, volar tilt, and articular incongruity. Follow-up radiographs should be reassessed for these variables, to ensure maintenance of the reduction, and should be searched for potential complications regarding fracture healing.

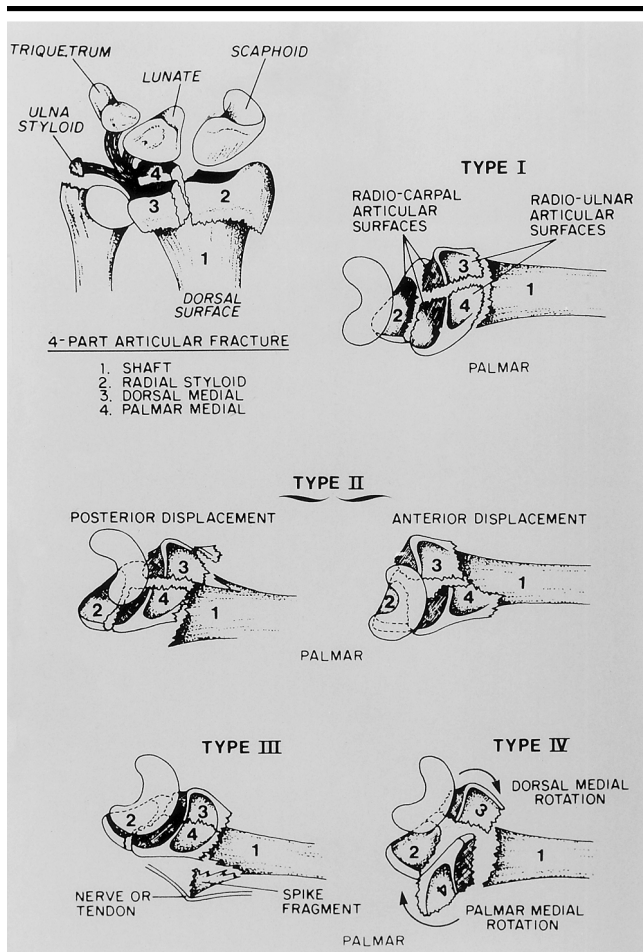


Figure 11. Diagrams show the Melone classification of distal radius fractures. (Reprinted, with permission, from reference 29.)

CARPAL FRACTURES

Carpal fractures, in general, are considerably less common than fractures of the distal radius, although scaphoid fractures are the second most common wrist injury (39–41). Scaphoid and triquetral fractures are far more common than are fractures to the other carpal bones. While fractures of the distal radius are challenging from a treatment perspective, identification of the injury is rarely difficult. Carpal fractures, however, can be a diagnostic challenge owing to their infrequency, as well as to the difficulty in visualizing these fractures on conventional radiographs. Although each carpal bone will be discussed individually, these fractures are often associated with fractures of other carpal bones and the distal radius. Perilunate fracture-dislocation injuries are beyond the scope of this discussion but must be considered whenever carpal injuries exist.

Scaphoid Fractures

The scaphoid is the most frequent site of carpal fracture and intercarpal ligament injury (42) (Fig 13). It articulates proximally with the radial styloid and the scaphoid fossa of the distal radius, distally with the trapezium and trapezoid, and on its ulnar aspect with the capitate and lunate. Radiographically identifiable structures include the distal pole, the volar tubercle located at the distal pole immediately proximal to the trapezium, the waist, and the proximal pole. All of these structures may be identified on conventional radiographs obtained in planes other than only the PA or lateral.

An understanding of the vascular supply of the scaphoid is important for any discussion of scaphoid fractures. The internal vascularity of the scaphoid originates predominantly dorsally, entering the scaphoid at its waist and accounting for 70%–80% of the scaphoid's internal vascularity

(43). This dorsal supply is the major supply to the proximal pole, although minimal perfusion may be achieved through the scapholunate interosseous ligament or the radioscapheolunate ligament. A palmar arterial supply, entering the distal pole in close proximity to the distal tubercle, accounts for the remainder of the blood supply. Because the blood supply of the scaphoid is predominantly intraosseous and oriented in a distal-to-proximal orientation, fractures of the scaphoid waist and proximal pole may interrupt this tenuous supply and predispose the proximal pole to avascular necrosis (AVN). Osteonecrosis is directly related to fracture position: Fractures of the middle third are associated with a 30% incidence of AVN, and fractures of the proximal fifth are associated with a nearly 100% incidence of AVN (42) (Fig 14). Furthermore, the healing time of a more proximal scaphoid fracture will be prolonged owing to the poor vascularity of the proximal part of the scaphoid.

The mechanism of injury is most often due to hyperextension of the wrist, but it can also result from a pure compressive force. A fall on an outstretched hand causes palmar tensile and dorsal compressive force on the scaphoid. Cadaver study results have demonstrated that a large radial-sided force on an extended (95°–100°) wrist consistently reproduces a scaphoid fracture (44). A transverse loading injury, or pure compression force, may occur with automobile accidents and often leads to a stable fracture pattern. Of all fractures of the scaphoid, including those associated with intercarpal ligament injuries, 65% occur at the waist; 15%, at the proximal pole; 10%, through the distal body; 8%, through the volar tuberosity; and 2%, through the distal articular surface (45).

An appreciation of carpal kinematics will aid in the understanding of radiographic findings. Briefly, the scaphoid assumes a palmar-flexed, and thus foreshortened, attitude during radial deviation or wrist flexion. With ulnar deviation or wrist extension, the scaphoid extends and appears elongated on the PA radiograph. Disruption of the volar carpal ligaments and the scapholunate interosseous ligament, as occurs in perilunate dislocations, will allow the scaphoid to assume a flexed position and the lunate an extended position, with the wrist in neutral position. With an unstable scaphoid fracture, the distal fragment flexes in the palmar direction and moves with the distal carpal row, while the proximal fragment extends and moves with the lunate. This leads to the "hump-back" deformity of the scaphoid associated

with healed but formerly unstable angulated scaphoid fractures (46) (Fig 15).

Imaging assessment.—Our initial radiographic assessment of a suspected scaphoid injury includes acquisition of PA, lateral, external oblique, and "scaphoid" views (ie, PA radiograph centered on the scaphoid, with the wrist held in ulnar deviation). These radiographic views should demonstrate the majority of scaphoid fractures (48). A PA or a PA-oblique radiograph may also be obtained with a clenched fist or tube angled toward the elbow and with the wrist in ulnar deviation to accentuate scaphoid extension (Fig 16). This view may help to identify scapholunate widening or a fracture line not visible on a conventional PA radiograph. Since scaphoid fractures can be radiographically occult, strong clinical suspicion of a scaphoid fracture (based on mechanism of injury, pain in the anatomic snuffbox) should dictate initial treatment in the presence of a normal radiograph. The patient should be treated with thumb-spica cast immobilization and be reevaluated both clinically and radiographically after 2 weeks. If clinical suspicion remains high despite normal radiographs, the clinician has two options. First, the cast can be replaced and the patient reexamined in 2 weeks. This avoids the costs of radiographic evaluation but may add to patient morbidity. Second, technetium 99 bone scintigraphy, MR imaging, or CT may be performed for a definitive evaluation of the scaphoid. Another approach to the possible occult scaphoid fracture is the use of MR imaging at the time of presentation when conventional radiographs are normal. Early use of MR imaging may prove to be cost-effective if immediate confirmation of the presence of a scaphoid fracture would affect the patient's returning to or staying away from work when costs of staying away from work are considered (47).

MR imaging has the advantage of demonstrating fractures not seen on conventional radiographs and allowing clarification of the abnormality within the scaphoid bone (15). CT can be performed in two planes, the coronal and long sagittal axis of the scaphoid, and will help identify and define displaced fractures of the scaphoid (14). Coronal CT sections of the hand and/or wrist can be obtained in most patients by placing the patient prone on the table, flexing the elbow 90°, placing the hand ulnar side down above the patient's head on the imaging table, and passing the CT beam parallel to the dorsum of the wrist. Alternatively, with

the patient prone on the table and the wrist palm side down, the hand and wrist can be elevated at a 30°–45° angle on the table. The wrist is extended and the gantry is angled so that CT sections are acquired parallel to the dorsal (or volar) surfaces of the scaphoid for coronal sections through the long axis of the scaphoid (14).

CT sections through the long sagittal axis of the scaphoid can be obtained by placing the wrist palm down (prone) on the CT tabletop with the hand, wrist, and forearm placed at about a 45° angle to the long axis of the CT tabletop. Anatomically, this alignment can be recognized by identifying the base of the thumb and the hard bone prominence on the middle portion of the distal radius (Lister tubercle). Alignment of these two points with the CT sections will suffice to produce CT sections at or near the long sagittal plane axes. These techniques, plus other variations of these techniques, are described by Stewart and Gilula (14). Thin sections can clearly demonstrate trabecular cortical detail for fragmentation or subtle cortical defects. Bone scintigraphy shows increased uptake at the fracture site and can potentially show decreased uptake over the proximal scaphoid fragment, which has decreased vascularity, and possible AVN in the proximal fragment (50), but scintigraphy provides minimal other information about the fracture with regard to displacement or angulation between fracture fragments. Scintigraphy cannot help distinguish bone marrow edema or bone bruise from a definite fracture.

Radiographic evaluation of suspected early-stage proximal-pole AVN is poor in that it is not sensitive. Sclerosis of the proximal pole may be observed but correlates poorly with AVN, because most patients with this condition simply have transient diminished vascularity to the proximal scaphoid pole, which causes less bone resorption (osteopenia) than in the distal part of the scaphoid. The relatively denser proximal part of the scaphoid usually recovers without scaphoid collapse (51). In general, with increased density of the proximal pole of the scaphoid during healing, when displacement of fracture fragments or fragmentation of the proximal pole is not developing and healing of the fracture site is occurring, we have been content to follow the fracture longer for healing. Increased clinical suspicion based on the radiographic and clinical findings should help determine the necessity and timing of MR imaging. Surgical concern about the proximal pole because of increasing pain while in a cast or developing nonunion that raises the question of performing sur-

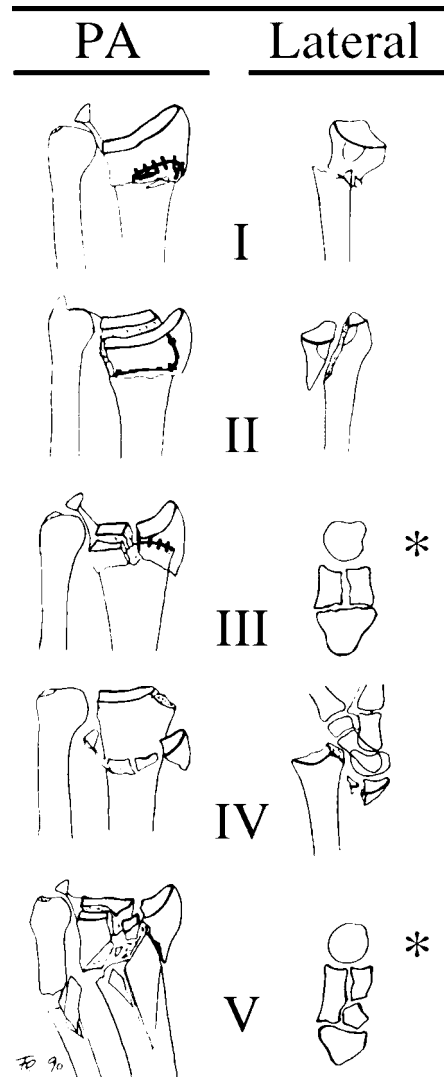


Figure 12. Diagrams show the five types of distal radius fractures described by Fernandez and Jupiter. (See text for specific information regarding each type.) On the lateral drawings, dorsal is to the reader's right. * = transverse (end-on) view of distal radius and ulna. Type I is a metaphyseal bending fracture. One cortex fails in tension, and the opposite fails in compression (eg, Smith fracture and Colles fracture). Type II is a shear fracture of the joint surface (Barton fracture). Type III is a compression fracture of the joint surface. Type IV is an avulsion fracture, usually associated with ligamentous injury. Type V is a high-energy injury, usually the result of a combination of mechanisms and forces. (Modified and reprinted, with permission, from reference 30.)

gical fusion are reasons for further evaluation of the dense proximal pole of the scaphoid.

Bone scintigraphy, CT, and MR imaging with gadolinium enhancement may all be helpful in the evaluation of suspected AVN. Determination of vascularity of the proximal pole of the scaphoid is



Figure 13. Scaphoid fracture. PA radiograph of the left wrist demonstrates a transverse fracture of the scaphoid waist. The fracture line (arrow) is visible at the capitate articular surface.

a critical piece of information for the hand surgeon. Gadolinium enhancement can further help in the MR evaluation of the proximal pole blood supply (52–54). Finally, surgeons (including the surgeon authors of this article and others) routinely evaluate vascularity in the operating room by searching for punctate bleeding in the scaphoid fracture fragments.

Radiographic assessment of scaphoid fractures and associated instability patterns are dependent on fracture identification and the measurement of several helpful angles. The entire scaphoid may be difficult to outline on conventional radiographs, however; CT performed along the long axis of the scaphoid can better demonstrate the shape of the scaphoid. Humpback deformity (46), common with both nonunion and malunion, is associated with increased angulation between the proximal and distal portions of the scaphoid as seen on the lateral radiographs or sagittal CT and MR imaging projections (55). The capitolunate angle is also measured on the lateral radiograph. This angle is measured between the long axis of the capitate and the midplane axis of the lunate and should be less than 30°. If the lunate is tilted dorsally more than normal in the presence of a scaphoid fracture, there is a strong suggestion of dorsal tilting of the proximal scaphoid fragment (46). Finally, the scapholunate angle is measured on the lateral radiograph. This angle is measured between the long axis of the scaphoid and the midplane axis of the lunate and should normally be 30°–60°. An angle of greater than 80° or less than 30° usually

indicates an instability pattern or dorsal tilting of the proximal scaphoid fracture fragment (46). These measurements, together with the fracture pattern, help classify the fractures and guide treatment. Radiographs of the contralateral wrist are often valuable, because there is a large range of normal variation in these measurements. Also, to perform these measurements, the dorsum of the metacarpals and the distal radius should be placed in a straight line on lateral radiographs and the scaphopisocapitate relationship (12) should be maintained.

Classification.—Several fracture classification systems have been proposed for the documentation of scaphoid fracture. The Russe classification system (56) describes the fracture on the basis of orientation: horizontal oblique, vertical oblique, or transverse (Fig 17). Vertical oblique fractures were thought to be the least stable and most likely to require surgical intervention. Cooney et al (57) proposed that scaphoid fractures be considered as either nondisplaced or displaced. Herbert (58) proposed a more detailed classification scheme (Fig 18). In the Herbert classification, displacement or instability of a scaphoid fracture is defined as displacement of the fragment by at least 1 mm or angulation shown by a radiolunate angle of more than 15° or a scapholunate angle of more than 60°. Because each of these classifications emphasizes a particular aspect of the fracture, the radiologist should fully characterize the fracture and include the orientation of the fracture, displacement, and angulation. If the above information is provided, the orthopedic surgeon can apply any classification scheme for treatment purposes.

Treatment.—The appropriate acute treatment of the scaphoid fracture remains controversial. Potential surgical intervention may be modified on the basis of the patient's hand dominance, level of demand, associated injuries, and location of the scaphoid fracture. Patient factors notwithstanding, nondisplaced stable fractures can be treated with a thumb-spica cast, with healing rates approaching 95% (48). Healing times for appropriately immobilized wrists average 8–12 weeks for the nondisplaced fracture. A scaphoid fracture is not considered united until it has been documented with progressive loss of fracture line visibility on conventional radiographs or coronal and sagittal CT sections. If increased radiolucency develops along a fracture line or if a round or oval focal area of radiolucency develops at the waist of the scaphoid, motion along a scaphoid fracture line should be suspected. Fracture frag-

ment alignment should be followed closely on PA and lateral views, with verification that the lateral views are positioned symmetrically at each follow-up examination. Use of the scaphopisocapitate criterion mentioned earlier can be of great help for the recognition of acceptable lateral views of the wrist. When healing of the fracture site is uncertain or must be verified better than can be accomplished with conventional radiographs, thin CT sections in the coronal and long scaphoid sagittal planes can be helpful (14). CT is especially helpful when evaluating a carpus that is still in a cast.

Although thumb-spica cast immobilization is accepted as the treatment of choice for scaphoid fractures, controversy exists as to whether immobilization should extend above the elbow. A thumb-spica cast decreases the forces transmitted along the first metacarpal-trapezial axis and provides increased stability to the scaphoid. Some clinicians, however, suggest that the thumb need not be immobilized, and below-the-elbow cast immobilization alone, with the wrist in neutral deviation and flexion/extension, is all that is required (59). Decreased time to union and reduced rates of nonunion have been demonstrated after treatment with a long arm cast when compared with those after treatment with a short arm-spica cast (59). Another deforming force on the distal scaphoid pole is the palmar radioscaphecapitate ligament, and the purpose of immobilization should be to attempt to relax this ligament (44). Thus, spica immobilization should be positioned with slight palmar flexion and radial deviation with a long arm spica cast (59).

Unstable fractures have an estimated 50% nonunion rate after nonsurgical treatment, because of carpal instability associated with these fractures (60). This rate is due to associated ligament disruptions or persistent motion, angulation, and displacement between scaphoid fracture fragments. Even with healing, there is an increased incidence of malunion and late collapse. Surgical treatment is usually undertaken for these fractures. Many modes of surgical fixation are appropriate. Kirschner wires, Herbert screws (a headless screw with proximal and distal threads of different pitch, designed to provide compression), and Herbert-Whipple screws (similar to Herbert screws, but central cannulation of the Herbert-Whipple screws allows introduction of the screw over a guide wire) can be used. All are inserted with fluoroscopic guidance. The standard AO cancellous screw may achieve satisfactory fixation as well. After reduction, the same



a.



b.

Figure 14. Osteonecrosis of the scaphoid. (a) PA radiograph of the left wrist demonstrates a transverse fracture at the proximal third of the scaphoid (black arrows) and fragmentation of the proximal fracture fragment (white arrow). The distal fragment appears sclerotic, but this is due to foreshortening of the scaphoid, with its distal pole overlapping its waist. (b) PA fluoroscopic spot view of the same wrist with ulnar deviation. The proximal articular surface is irregular, with a mixture of sclerosis and lysis. Part of the proximal subchondral bone cortex has disappeared (arrows). The distal portion of the scaphoid has normal mineralization.

analysis of fracture fragment alignment as mentioned earlier should be performed. Comparison with preoperative radiographs is valuable to check for more anatomic alignment. At times, CT may be necessary to confirm fracture fragment location (14).

Aside from the acute fracture, two common clinical situations of failed conservative treatment and delayed presentation are important. Patients may present 3–6 months after initial scaphoid injury if symptoms are mild; treatment does not change, and nondisplaced fractures can be expected to heal, although time to union may be slightly prolonged. Failed conser-

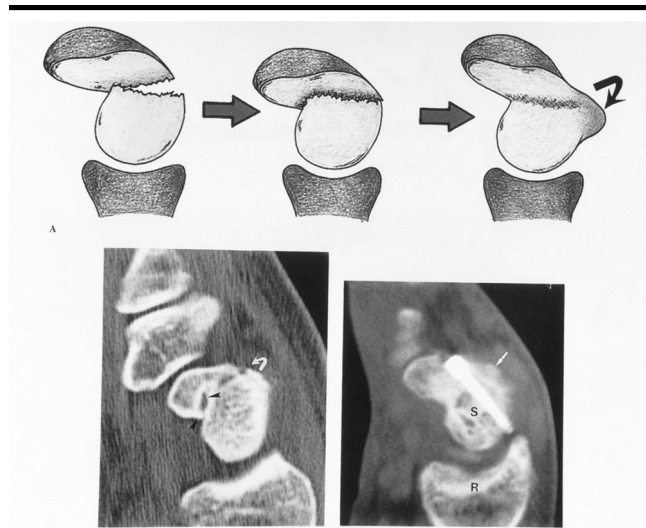


Figure 15. A, Drawings show development of the dorsal humpback deformity of the scaphoid after fracture of the scaphoid waist, with angulation between the proximal and distal scaphoid fracture fragments. At first, there is angulation between fragments; next, the two fragments settle or impact into each other; and finally an exostosis (curved arrow) or bony prominence (the humpback deformity) develops dorsally at the fracture site. B, Long-axis scaphoid CT image shows a developing dorsal humpback deformity (arrow). This deformity is caused by ventral angulation of the distal scaphoid fracture fragment and late exostosis formation at the fracture site dorsally. Nonunion is evident with cortical margins (arrowheads) along the ventral half of the fracture line. C, In another patient, who underwent internal fixation, exostosis (arrow) is developing dorsally on the scaphoid (S). R = radius. (Reprinted, with permission, from reference 47.)



a.



b.

Figure 16. Scaphoid fracture. (a) PA radiograph of the right wrist with ulnar deviation demonstrates a questionable fracture fragment (arrow) at the radial side of the scaphoid with otherwise normal appearance. (b) A 45° oblique radiograph of the right wrist with full ulnar deviation and tube angulation toward the elbow clearly demonstrates a transverse fracture line (arrows) at the scaphoid waist.

ative treatment warrants surgical intervention. There are a variety of surgical techniques for the treatment of nonunion

with bone grafting to restore the normal carpal alignment and ligamentous tension as the primary goal. Russe (56), Fiske (61),

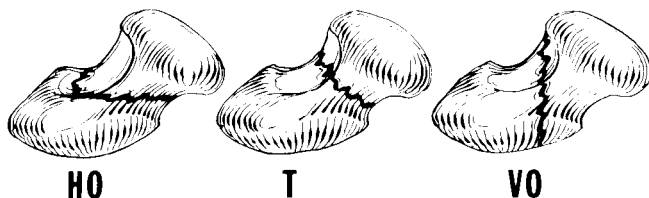


Figure 17. Diagrams show the Russe classification of scaphoid fractures, which include horizontal oblique (HO), transverse (T), and vertical oblique (VO) fractures. (Reprinted, with permission, from reference 7, p 806.)

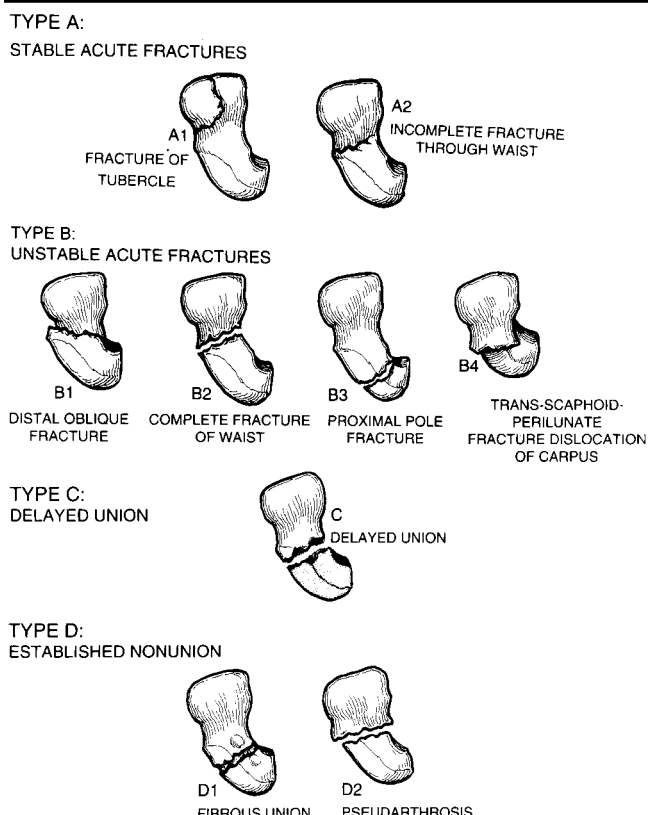


Figure 18. Diagrams show the Herbert classification of scaphoid fractures. (Reprinted, with permission, from reference 7, p 805.)

and Fernandez (62) have described techniques that can be effective in achieving union. Vascularized grafts may be used for AVN of the proximal pole associated with nonunion of the fracture. Recalcitrant nonunion or scapholunate advanced collapse may require radiocarpal or intercarpal fusion or proximal row carpectomy.

Scaphoid nonunion has been associated with the development of late arthritis of the wrist, and this pattern is commonly referred to as scaphoid nonunion advanced collapse, or SNAC (63). Displaced fractures typically progress to symptomatic arthritis more rapidly and more extensively than do nondisplaced fractures. Arthritis will involve the ra-

dioscaphoid joint 10–20 years after the injury and will involve the entire wrist after more than 20 years (64). Also, it has been noted that arthritis initially involves the scaphoid-radial-styloid articulation and eventually progresses to involve the scaphocapitate and capitolunate joints (SNAC wrist). Radiographic features include marked osteoarthritis of the radioscaphoid joint, with radial styloid involvement and loss of normal scaphoid shape. With fractures of the waist or proximal third of the scaphoid, the joint space between the radius and the proximal scaphoid fragment typically is preserved. In other words, the proximal scaphoid fracture fragment acts like a small lunate.

The radiolunate joint is consistently spared from the degenerative changes (63,65). These reports emphasize the need to achieve anatomic reduction and union of scaphoid fractures (66).

Lunate Fractures

Lunate injuries (40,41,67) are generally associated with a fall on an outstretched wrist; a compression force may also be involved. The position of the carpus at impact determines the specific injury. Avulsion injuries of the volar pole of the lunate or the proximal radial corner of the triquetrum are likely associated with perilunate dislocations or other ligamentous injuries about the lunate.

Lunate fractures may be overlooked in the acute setting because of the difficulty in recognition of these injuries on conventional radiographs. The initial series of radiographs remains the standard PA, the PA with ulnar deviation, oblique, and lateral views. The dorsal cortical lines of the distal radius, the scaphoid, and the triquetrum all typically overlap the lunate and make the identification of fractures difficult on PA images. Despite the overlapping of cortical structures by other carpal bones, however, all the margins of the lunate should be closely examined on all views to allow one to suspect or diagnose lunate fractures. On the lateral view, a break in the volar or dorsal cortex of the lunate may suggest a volar or dorsal fracture of the distal lunate. An accompaniment of volar perilunate subluxation or dislocation would support the diagnosis of translunate volar perilunate fracture subluxation or dislocation. A small radiopacity on the radial proximal edge of the lunate may indicate an osteophyte, such as may develop with abnormal motion at the scapholunate joint, or avulsion or posttraumatic change of the scapholunate ligament at its attachment to the lunate. “Double-density,” or additional radiopaque, lines in the proximal surface or radial or ulnar sides of the lunate may indicate a fracture in the lunate. Finally, depression or offset in the distal cortical concavity of the lunate as seen on lateral or frontal views can indicate a lunate fracture. With any questions about these findings, fluoroscopic spot images, CT scans, or MR images can help answer the question. When CT is performed, thin enough sections (typically 2-mm-thick sections at 1–2-mm intervals) to show subtle cortical offset must be obtained. Study results (68) have shown that MR imaging can demonstrate normal anatomy, as well as pathologic conditions, at intrinsic and extrinsic

ligaments. MR images have been found to correlate with histologic results from biopsies of the lunate (69). This makes scintigraphy, transverse and sagittal CT, and MR imaging all reasonable options for evaluation of the lunate if the clinical suspicion for lunate injury or other abnormality is high.

Kienböck disease, or AVN of the lunate, is believed by some to be a chronic manifestation of lunate fractures in which collapse of the lunate causes the late development of symptoms (70) (Fig 19). Therefore, all patients with lunate fractures warrant periodic follow-up for the development of AVN and symptomatic Kienböck disease.

Triquetrum Fractures

Triquetral fractures generally occur on the dorsal surface (Fig 4) (39–41) or, less commonly, involve the body (Fig 20) of the triquetrum. The dorsal surface of the triquetrum may be fractured by means of impingement from the ulnar styloid, shear forces, or avulsion from strong ligamentous attachments (39,40). The body also may be fractured, typically in a transverse pattern (39,40). A chip fracture off the radial proximal corner of the triquetrum may indicate a former perilunate fracture-dislocation. Such a chip fracture may be demonstrated better on CT or MR images and may be overlooked on conventional radiographs. If associated with a perilunate dislocation, other carpal fractures are common and should not be overlooked. Transverse fractures are usually demonstrated on the PA radiograph, but dorsal avulsion injuries are best detected on a lateral projection. CT or MR images may be more sensitive than conventional radiographs for detection of avulsion injuries. Surgical intervention is rarely required, but a persistently symptomatic chip fracture may require excision (39). Recognition of a perilunate fracture-subluxation or fracture-dislocation pattern that may have reduced itself (as in patients with an avulsion fracture off the proximal volar radial edge of the triquetrum or the volar distal pole of the lunate or with fractures of the waist of the scaphoid and capitate) may lead to surgical fixation.

Trapezium Fractures

Fractures of the trapezium (39–41) are most commonly transverse loading injuries in the setting of an adducted thumb in which the first metacarpal is driven into the trapezium (Fig 21). The standard

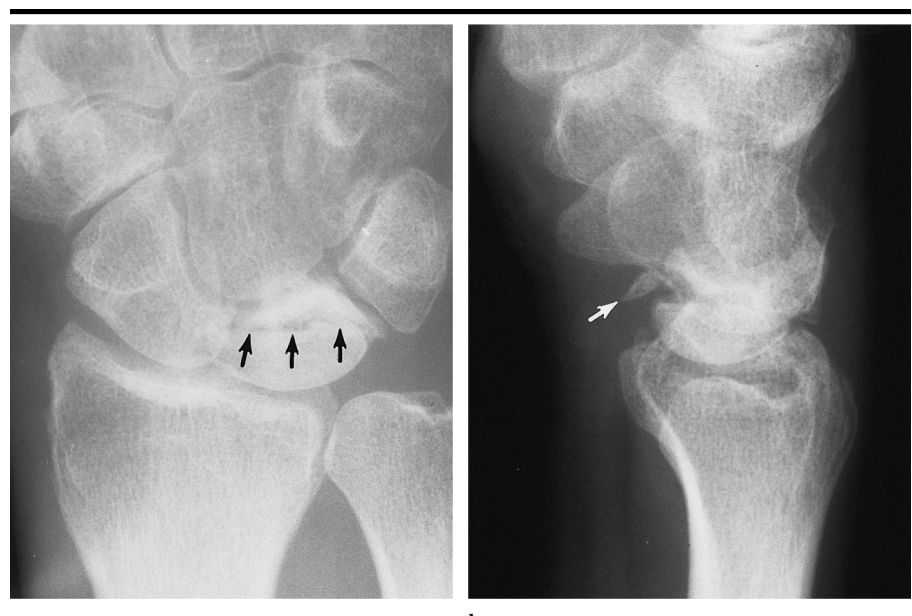


Figure 19. Kienböck disease. (a) PA radiograph of the right wrist demonstrates increased sclerosis of the lunate with fragmentation. A transverse fracture line (arrows) through the lunate with a sclerotic margin is present, and the distal fracture fragment has migrated toward the ulna. (b) Lateral radiograph of the same wrist further demonstrates sclerotic changes and fragmentation of the lunate. A separate fracture fragment (arrow) is present in a volar location.



Figure 20. Triquetral fracture. (a) PA radiograph of the right wrist demonstrates a vertical fracture line (arrows) located at the radial third of the triquetrum. (b) A 45° oblique radiograph of the right wrist demonstrates the same fracture line (arrows), with 1-mm separation between the fracture fragments.

radiographic examination will usually demonstrate this fracture. Trapezial fractures are often associated with a fracture of the first metacarpal base and/or subluxation or dislocation of the first carpo-metacarpal joint (40). The resulting fracture is longitudinal and intraarticular. This fracture is often due to high-energy impact and may be associated with wrist injuries, including fractures of the distal radius. Displaced fractures may require open reduction and internal fixation,

typically performed with Kirschner wires or screws.

The transverse carpal ligament may cause a volar-trapezial ridge avulsion injury (71,39,40). Carpal tunnel views are helpful in attempts to outline this fracture, but CT may also be necessary for fracture definition. These injuries may involve the base or the tip of the trapezial ridge. These fractures typically heal or become asymptomatic and only rarely necessitate fragment excision because of



a. b.

Figure 21. Trapezial fracture. (a) PA radiograph of the right wrist demonstrates a transverse fracture line (arrows) through the proximal third of the trapezium, with approximately 2-mm ulnar displacement of the distal fracture fragment. (b) Lateral radiograph of the same wrist demonstrates 2-mm separation (arrow) between the fracture fragments of the trapezium.



a. b.

Figure 22. Hamate fracture. (a) PA radiograph of the right wrist demonstrates an oblique fracture line (arrows) at the distal ulnar third of the hamate, with 0.5-mm separation of the ulnar fracture fragment. (b) A 45° oblique radiograph of the same wrist demonstrates the hamate fracture (arrow), with 2–3 mm of distal and dorsal displacement of the fracture fragment.

persistent pain (39,40). An additional trapezial fracture that is easy to miss is the fracture off the dorsoulnar tubercle of the distal surface of the trapezium (72). Patients with this fracture present with pain at the junction of the bases of the first and second metacarpals. Recognition of the fracture may require acquisition of tomograms, CT scans, or MR images. Bone scintigraphy is also valuable for evaluation of this area of the trapezium. Once detected, treatment with cast placement or splinting can be successful (72).

Pisiform Fractures

The pisiform is a sesamoid bone within the insertion of the flexor carpi ulnaris tendon and is subjected to large stresses. Pisiform bone injury often occurs in the setting of a direct blow (39–41). The injury may be a vertical or transverse fracture (linear or comminuted) or a compression injury. These fractures may be difficult to detect on standard radiographs, and a carpal tunnel or pisotriquetral radiograph or CT or MR images are

often needed. This fracture may be associated with other upper-extremity fractures, resulting in delayed recognition and treatment. Cast immobilization is the standard treatment, but chronic pain, usually related to malunion or nonunion, may develop. Pisiform excision is an option for persistent discomfort and is effective in relieving symptoms (73).

Hamate Fractures

Hamate injuries are typically of two varieties (39–41,74). First, there may be a transverse loading injury with a dorsally displaced articular fracture (Fig 22). These may be associated with an ulnar-sided metacarpal fracture and fourth and fifth carpometacarpal dislocation. CT performed in transverse plus coronal and sagittal planes can help clearly define the presence of these fractures, displacements, and fracture-subluxations. These injuries typically heal or become asymptomatic with cast immobilization (39). Displaced intraarticular fractures of the hamate may involve the fourth or fifth carpometacarpal joints, requiring open reduction and fixation with Kirschner wires (40).

The hook of the hamate can be injured by means of direct trauma, typically a direct blow (40), or avulsive force through the transverse carpal ligament. This avulsion injury is associated with racquet sports and golf (39,40). Diagnosis requires a high index of suspicion, and pain at direct palpation is a clinical hallmark. A carpal tunnel radiograph, a 20° supine oblique view; a reversed oblique (overpronation) view; or a radial, deviated, lateral, thumb-abducted view (75) are helpful conventional radiographic projections for help in the detection of these injuries (Fig 23). CT in the transverse plane or MR imaging can also show these fractures if questions remain about the presence or position of a hamate hook fracture (14).

The os hamulus proprius, an unfused ossification center, may mimic an old fracture, because both are peripherally corticated; however, the os hamulus proprius is usually much larger than an avulsion of the hamate hook (76). However, there generally is no difficulty differentiating these two entities, because the os hamulus proprius is usually larger than the adjacent base of the hamate hook and may have a different shape than the normal hook. Untreated fractures may progress to nonunion, and, rarely, symptomatic nonunions will require excision of the hook of the hamate for symptomatic relief (40,77).



a.



b.



c.

Figure 23. Hamate hook fracture. (a) PA radiograph of the right wrist demonstrates a normal-appearing wrist. (b) Lateral radiograph of the same wrist demonstrates no fracture. (c) Carpal tunnel radiograph of the same wrist demonstrates an oblique fracture (arrow) of the hook of the hamate.

Capitate Fractures

Capitate fractures are another rare type of injury (40,41), and diagnosis requires a high index of suspicion based on the mechanism of injury or clinical examination findings (Fig 24). Demonstration of capitate fractures may require angled-beam radiographs, as can be performed with angled fluoroscopic spot imaging. CT and MR imaging can be used to demonstrate the fracture. However, because CT must be planned to acquire sections at right angles to the fracture line, MR imaging has the advantage over CT to show abnormal marrow signal intensity, as well as the fracture line, if images in multiple planes are obtained. MR imaging is also helpful in eval-

uating for AVN. Typically, these capitate waist fractures are nondisplaced fractures that heal uneventfully; however, the proximal pole of the capitate is similar to the scaphoid in that it is intraarticular and covered with hyaline cartilage. Consequently, fractures of the capitate waist may rarely progress to AVN of the proximal pole. Nonsurgical care is the treatment of choice even for advanced AVN, because patients often remain asymptomatic (40). A capitate waist fracture may accompany a scaphoid waist fracture and is then called the scaphocapitate syndrome (39,40,78). This likely represents a perilunate injury and requires open reduction and internal fixation (40).



a.



b.

Figure 24. Capitate fracture. (a) PA radiograph of the left wrist demonstrates a fracture line (arrows) at the proximal third of the capitate, with a widened gap at its ulnar side. (b) Lateral view of the same wrist demonstrates subtle dorsal tilting of the proximal fracture fragment (arrows), with a step-off at the palmar side of the cortex (top arrow).

Trapezoid Fractures

Fractures of the trapezoid are rare (40,41), owing to its stable articulations, especially with the second metacarpal, and are typically associated with dislocation. These injuries may be associated with a dislocation of the second metacarpal. Surgical intervention is rarely required (39). Generally, these fractures can be identified at conventional radiog-



a.



b.

Figure 25. Trapezoidal fracture. (a) PA radiograph of the right wrist demonstrates proximal migration of the second metacarpal bone with compression fracture (arrow) of the trapezoid. (b) Fluoroscopic spot view of the same wrist further demonstrates the trapezoid fracture (arrow) and proximal migration of the second metacarpal bone.

raphy (Fig 25), but subtle injuries may require CT or MR imaging for diagnosis. Indications for CT or MR imaging include focal tenderness over the trapezoid, swelling overlying this bone, and/or very high uptake over the trapezoid at bone scintigraphy. Closed reduction and cast or percutaneous pin immobilization are usually sufficient for treatment (39); however, large articular fragments may require open reduction and internal fixation (40,79).

CONCLUSION

Fractures of the distal radius and carpal bones are common and complex entities. A full understanding of fracture dynamics and treatment options is necessary to provide a concise yet complete radiographic evaluation. We have provided a detailed discussion of common wrist fractures, with an emphasis on what the orthopedic surgeon needs to know for treatment purposes.

References

- Owen RA, Melton LJ III, Johnson KA, Ilstrup DM, Riggs BL. Incidence of Colles' fracture in a North American community. *Am J Pub Health* 1982; 72:605-607.
- Catalano LW III, Cole RJ, Gelberman RH, Evanoff BA, Gilula LA, Borrelli J Jr. Displaced intra-articular fractures of the distal aspect of the radius. *J Bone Joint Surg Am* 1997; 79:1290-1302.
- DePalma AF. Comminuted fractures of the distal end of the radius treated by ulnar pinning. *J Bone Joint Surg Am* 1952; 34:651-662.
- Kihara H, Palmer AK, Werner FW, Short WH, Fortino MD. The effect of dorsally angulated distal radius fractures on distal radioulnar joint congruency and forearm rotation. *J Hand Surg Am* 1996; 21:40-47.
- Pogue DJ, Viegas SF, Patterson RM, et al. Effects of distal radius fracture malunion on wrist joint mechanics. *J Hand Surg Am* 1990; 15:721-727.
- Short WH, Palmer AK, Werner FW, Murphy DJ. A biomechanical study of distal radius fractures. *J Hand Surg Am* 1987; 12:529-534.
- Green DP. *Operative hand surgery*. 3rd ed. New York, NY: Churchill-Livingstone, 1993.
- Gilula LA, Weeks PM. Post-traumatic ligamentous instabilities of the wrist. *Radiology* 1978; 129:641-651.
- Mayfield JK. *Wrist ligament anatomy and biomechanics*. In: Gilula LA, ed. *The traumatized hand and wrist: radiographic and anatomic correlation*. Philadelphia, PA: Saunders, 1992; 242.
- Gilula LA. Carpal injuries: analytic approach and case exercises. *AJR Am J Roentgenol* 1979; 133:503-517.
- Jedlinski A, Kauer JMG, Jonsson K. X-ray evaluation of the true neutral position of the wrist: the groove for extensor carpi ulnaris as a landmark. *J Hand Surg Am* 1995; 20:511-512.
- Yang Z, Mann FA, Gilula LA, Haerr C, Larsen CF. Scaphopisocapitate alignment: criterion to establish a neutral lateral view of the wrist. *Radiology* 1997; 205:865-869.
- Pruitt DL, Gilula LA, Manske PR, Vannier MW. Computed tomography scanning with image reconstruction in evaluation of distal radius fractures. *J Hand Surg Am* 1994; 19:720-727.
- Stewart NR, Gilula LA. CT of the wrist: a tailored approach. *Radiology* 1992; 183: 13-20.
- Breitenseher MJ, Metz VM, Gilula LA, et al. Radiographically occult scaphoid fractures: value of MR imaging in detection. *Radiology* 1997; 203:245-250.
- Yin Y, Wilson AJ, Gilula LA. Three-compartment wrist arthrography: direct comparison of digital subtraction with non-subtraction images. *Radiology* 1995; 197: 287-290.
- Mann FA, Wilson AJ, Gilula LA. Radiographic evaluation of the wrist: what does the hand surgeon want to know? *Radiology* 1992; 184:15-24.
- Baratz ME, Larsen CF. Wrist and hand measurements and classification schemes. In: Gilula LA, Yin Y, eds. *Imaging of the wrist and hand*. Philadelphia, PA: Saunders, 1996; 232.
- Mann FA, Kang SW, Gilula LA. Normal palmar tilt: is dorsal tilting really normal? *J Hand Surg Br* 1992; 17:315-317.
- Colles A. The classic: on the fracture of the carpal extremity of the radius (reprinted from original 1814 article). *Clin Orthop* 1972; 83:3-5.
- Peltier LF. Eponymic fractures: Robert William Smith and Smith's fracture. *Surgery* 1959; 45:1035-1042.
- Barton JR. Views and treatment of an important injury to the wrist. *Med Examiner* 1838; 1:365-368.
- Edwards HC. The mechanism and treatment of backfire fracture. *J Bone Joint Surg* 1926; 8:701-717.
- Scheck M. Long term follow-up of treatment of comminuted fractures of the distal end of the radius by transfixation with Kirschner wires and cast. *J Bone Joint Surg Am* 1962; 44:337-351.
- Peh WCG, Gilula LA. Normal disruption of carpal arcs. *J Hand Surg Am* 1996; 21: 561-566.
- Anderson DJ, Blair WF, Steyers CM Jr, Adams BD, El-Khoury GY, Bhandari EA. Classification of distal radius fractures: an analysis of interobserver reliability and intraobserver reproducibility. *J Hand Surg Am* 1996; 21:574-582.
- Hauck RM, Skatien J, Palmer AK. Classification and treatment of ulnar styloid nonunion. *J Hand Surg Am* 1996; 21:418-422.
- Frykman G. Fracture of the distal radius including sequelae: shoulder-hand-finger syndrome, disturbance in the distal radio-ulnar joint and impairment of nerve function—a clinical and experimental study. *Acta Orthop Scand* 1967; 108(suppl):1-153.
- Melone CP Jr. Open treatment for displaced articular fractures of the distal radius. *Clin Orthop* 1986; 202:103-111.
- Fernandez DL. Fractures of the distal radius: operative treatment. In: Heckman JD, ed. *Instructional course lectures*. Vol 42. Rosemont, Ill: American Academy of Orthopaedic Surgeons, 1993; 73-88.
- Jupiter JB, Fernandez DL. Comparative classification for fractures of the distal end of the radius. *J Hand Surg Am* 1997; 22:563-571.
- Weber SC, Szabo RM. Severely comminuted distal radial fracture as an unsolved problem: complications associated with external fixation and pins and plaster techniques. *J Hand Surg Am* 1986; 11: 157-165.
- Axelrod T, Paley D, McMurtry RY. Limited open reduction of the lunate facet in comminuted, intra-articular fractures of the distal radius. *J Hand Surg Am* 1988; 13:372-377.
- Amadio PC, Botte MJ. Treatment of malunion of the distal radius. *Hand Clin* 1987; 3:541-561.
- Fernandez DL. Correction of post-traumatic wrist deformity in adults by osteotomy, bone grafting, and internal fixation. *J Bone Joint Surg Am* 1982; 64:1164-1178.
- Taleisnik J, Watson K. Midcarpal instability caused by malunited fractures of the distal radius. *J Hand Surg Am* 1984; 9:350-357.
- Palmer AK, Werner FW. Biomechanics of the distal radioulnar joint. *Clin Orthop* 1984; 187:26-35.
- Knirk JL, Jupiter JB. Intra-articular frac-

- tures of the distal end of the radius in young adults. *J Bone Joint Surg Am* 1986; 68:647-659.
39. Bryan RS, Dobyns JH. Fractures of the carpal bones other than lunate and navicular. *Clin Orthop Rel Res* 1980; 149:107-111.
40. Cohen MS. Fractures of the carpal bones. *Hand Clin* 1997; 13:587-599.
41. Razemon JP. Fractures of the carpal bones with the exception of fractures of the scaphoid. In: Razemon JP, Fisk GR, eds. *The wrist*. Edinburgh, Scotland: Churchill-Livingstone, 1988; 126-129.
42. Dobyns JH, Linscheid RL. Fractures and dislocations of the wrist. In: Rockwood CA Jr, Green DP, eds. *Fractures in adults*. 3rd ed. Philadelphia, Pa: Lippincott, 1984; 411-509.
43. Gelberman RH, Gross MS. The vascularity of the scaphoid bone. *J Hand Surg Am* 1980; 5:508-513.
44. Weber ER, Chao EY. An experimental approach to the mechanism of scaphoid waist fractures. *J Hand Surg Am* 1978; 3:142-148.
45. Cooney WP, Linscheid RL, Dobyns JH. Fractures and dislocations of the wrist. In: Rockwood CA Jr, Green DP, eds. *Fractures in adults*. 4th ed. Philadelphia, Pa: Lippincott, 1996; 745-867.
46. Smith DK, Gilula LA, Amadio PC. Dorsal lunate tilt (DISI configuration): sign of scaphoid fracture displacement. *Radiology* 1990; 176:497-499.
47. Yin YM, McEnergy KW, Gilula LA. Computed tomography. In: Gilula LA, Yin YM, eds. *Imaging of the wrist and hand*. Philadelphia, Pa: Saunders, 1996; 425.
48. Dickson RA, Leslie IJ. Conservative treatment of the fractured scaphoid. In: Razemon JP, Fisk GR, eds. *The wrist*. Edinburgh, Scotland: Churchill-Livingstone, 1988; 80-87.
49. Gaebler C, Kukla C, Breitenseher M, Trattagia S, Mittboeck M, Vecsei V. Magnetic resonance imaging of occult scaphoid fracture. *J Trauma* 1996; 41:73-76.
50. Bellmore MC, Cummie JL, Crocker RF, Canseldine DB. The role of bone scans in the assessment of prognosis of scaphoid fracture. *Aust N Z J Surg* 1983; 53:133-137.
51. Green DP. The effect of avascular necrosis on Russe bone grafting for scaphoid non-union. *J Hand Surg Am* 1985; 10:597-605.
52. Munk PL, Lee MJ, Janzen DL, et al. Gadolinium-enhanced dynamic MRI of the fractured carpal scaphoid: preliminary results. *Australas Radiol* 1998; 42:10-15.
53. Kulkarni RW, Wollstein R, Tayar R, Citron N. Patterns of healing of scaphoid fractures: the importance of vascularity. *J Bone Joint Surg Br* 1999; 81:85-90.
54. Schmitt R, Heinze A, Fellner F, Obbleter N, Struhn R, Bautz W. Imaging and staging of avascular osteonecrosis at the wrist and hand. *Eur J Radiol* 1997; 25:92-103.
55. Amadio PC, Berquist TH, Smith DK, Ilstrup DM, Cooney WP, Linscheid RL. Scaphoid malunion. *J Hand Surg Am* 1989; 14:679-687.
56. Russe O. Fracture of the carpal navicular: diagnosis, non-operative treatment and operative treatment. *J Bone Joint Surg Am* 1985; 67:428-432.
57. Cooney WP, Dobyns JH, Linscheid RL. Fractures of the scaphoid: a rational approach to management. *Clin Orthop* 1980; 149:90-97.
58. Herbert TJ. The fractured scaphoid. St Louis, Mo: Quality Medical, 1990; 52.
59. Gellman H, Caputo RJ, Carter V, Aboulaafia A, McKay M. Comparison of short and long arm thumb-spica casts for nondisplaced fractures of the carpal scaphoid. *J Bone Joint Surg Am* 1989; 71:354-357.
60. Dabezies EJ, Matthews R, Faust DC. Injuries to the carpus: fractures of the scaphoid. *Orthopedics* 1982; 5:1510-1521.
61. Fiske GR. An overview of injuries of the wrist. *Clin Orthop* 1980; 149:137-144.
62. Fernandez DL. A technique for anterior wedge-shaped grafts for scaphoid non-unions with carpal instability. *J Hand Surg Am* 1984; 9:733-737.
63. Vender MI, Watson HK, Wiener BD, Black DM. Degenerative change in symptomatic scaphoid nonunion. *J Hand Surg Am* 1987; 12:514-519.
64. Mack GR, Bosse MJ, Gelberman RH, Yu E. The natural history of scaphoid non-union. *J Bone Joint Surg Am* 1989; 66: 504-509.
65. Watson HK, Ballet FL. The SLAC wrist: scapholunate advanced collapse pattern of degenerative arthritis. *J Hand Surg Am* 1984; 9:358-365.
66. Ruby LK, Stinson J, Belsky MR. The natural history of scaphoid non-union: a review of fifty-five cases. *J Bone Joint Surg Am* 1985; 67:428-432.
67. Teisen H, Hjarback J. Classification of fresh fractures of the lunate. *J Hand Surg Br* 1988; 13:458-462.
68. Totterman SM, Miller R, Wasserman B, Blebea JS, Rubens DJ. Intrinsic and extrinsic carpal ligaments: evaluation by three-dimensional Fourier transform MR imaging. *AJR Am J Roentgenol* 1993; 160:117-123.
69. Trumble TE, Irving L. Histologic and magnetic resonance imaging correlations in Kienbock's disease. *J Hand Surg Am* 1990; 15:879-884.
70. Beckenbaugh RD, Shives TC, Dobyns JH, Linscheid RL. Kienbock's disease: the natural history of Kienbock's disease and consideration of lunate fractures. *Clin Orthop* 1980; 149:98-106.
71. Mayfield JK, Gilula LA, Totty WG. Multiple carpal fractures. In: Gilula LA, ed. *The traumatized hand and wrist: radiographic and anatomic correlation*. Philadelphia, Pa: Saunders, 1992; 269.
72. Griffin AC, Gilula LA, Young VL, Strecker WB, Weeks PM. Fracture of the dorsoulnar tubercle of the trapezium. *J Hand Surg Am* 1988; 13:622-626.
73. Palmieri TJ. The excision of painful pisiform bone fractures. *Orthop Rev* 1982; 11:99-103.
74. Milch H. Fracture of the hamate bone. *J Bone Joint Surg* 1934; 16A New Series(32A Old Series):459-462.
75. Bhalla S, Higgs PE, Gilula LA. Utility of the radial-deviated, thumb-abducted lateral radiographic view for the diagnosis of hamate hook fractures: case report. *Radiology* 1998; 209:203-207.
76. Schmidt H, Freyschmidt L, eds. *Arm: carpal bones*. In: *Borderlands of normal and early pathologic findings in skeletal radiology*. New York, NY: Thieme, 1993; 102-105.
77. Bishop AT, Beckenbaugh RD. Fracture of the hamate hook. *J Hand Surg Am* 1988; 13:135-139.
78. Fenton RL. The naviculo-capitate fracture syndrome. *J Bone Joint Surg Am* 1956; 38:681-684.
79. Pruzansky M, Arnold L. Delayed union of fractures of the trapezoid and body of the hamate. *Orthop Rev* 1987; 16:36-40.